Supporting information

Modified Separator Performing Dual Physical/Chemical Roles to Inhibit Polysulfide Shuttle Resulting in Ultra-Stable Li–S Batteries

Syed Ali Abbas[†‡□], Jiang Ding[§□], Sheng Hui Wu[¶], Jason Fang[¶], Karunakara Moorthy Boopathi[□], Anisha Mohapatra[†‡□], Li Wei Lee[±], Pen-Cheng Wang[†], Chien-Cheng Chang[§], Chih Wei Chu*[□ǂ]

[†] Department of Engineering and Systems Science, National Tsing Hua University. Hsinchu 30013, Taiwan

[‡] Nano Science and Technology Program, Taiwan International Graduate Program, Academia Sinica, National Tsing Hua University, Taiwan

[□] Research Center of Applied Sciences, Academia Sinica Taipei 115, Taiwan

[§] Institute of Applied Mechanics, National Taiwan University, 1 Sec. 4, Roosevelt Road, Taipei 106, Taiwan

[¶] Material and Chemical Research Laboratories, Industrial Technology Research Institute, Hsinchu, 31040, Taiwan

[±] Institute of Chemistry, Academia Sinica, Taipei 115, Taiwan

[ǂ] College of Engineering, Chang Gung University, Taoyuan 33302, Taiwan

*To whom correspondence should be addressed: E-mail gchu@gate.sinica.edu.tw; Web: http://www.rcas.sinica.edu.tw/faculty/gchu.html

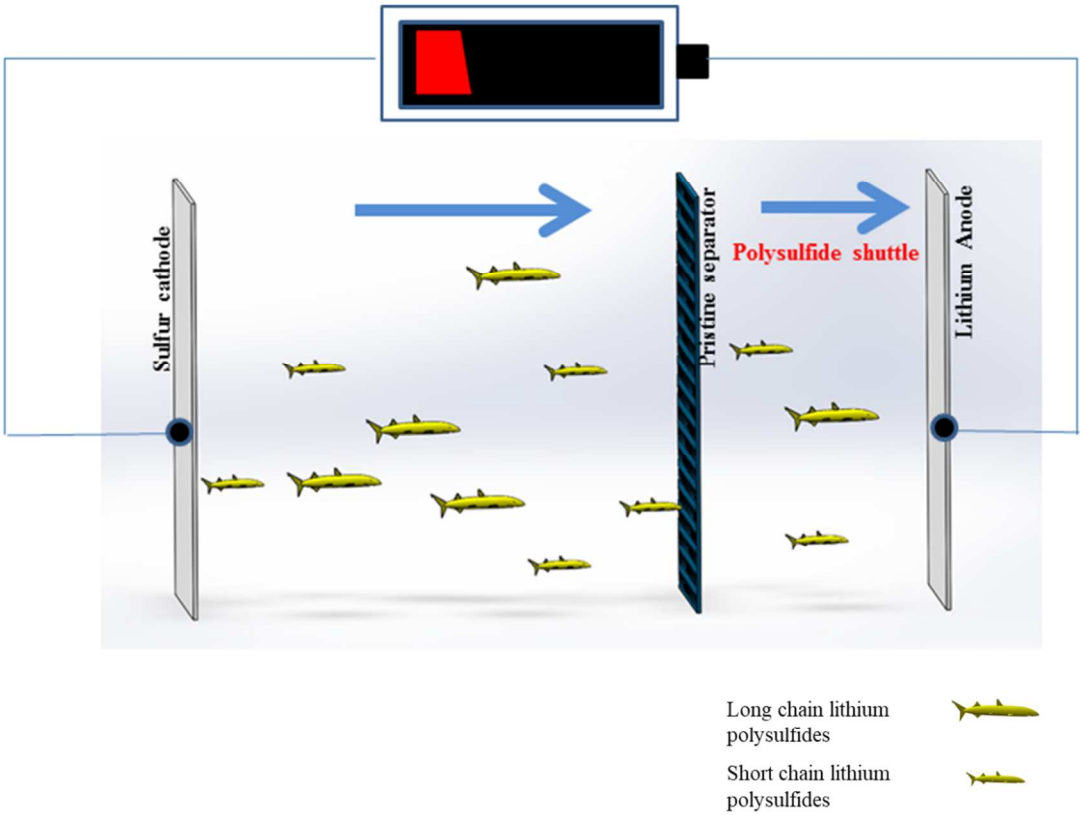

Figure S1. Schematic representation of the discharge mechanism of the Li–S cell, illustrating the diffusion of LiPSs when using the pristine separator.

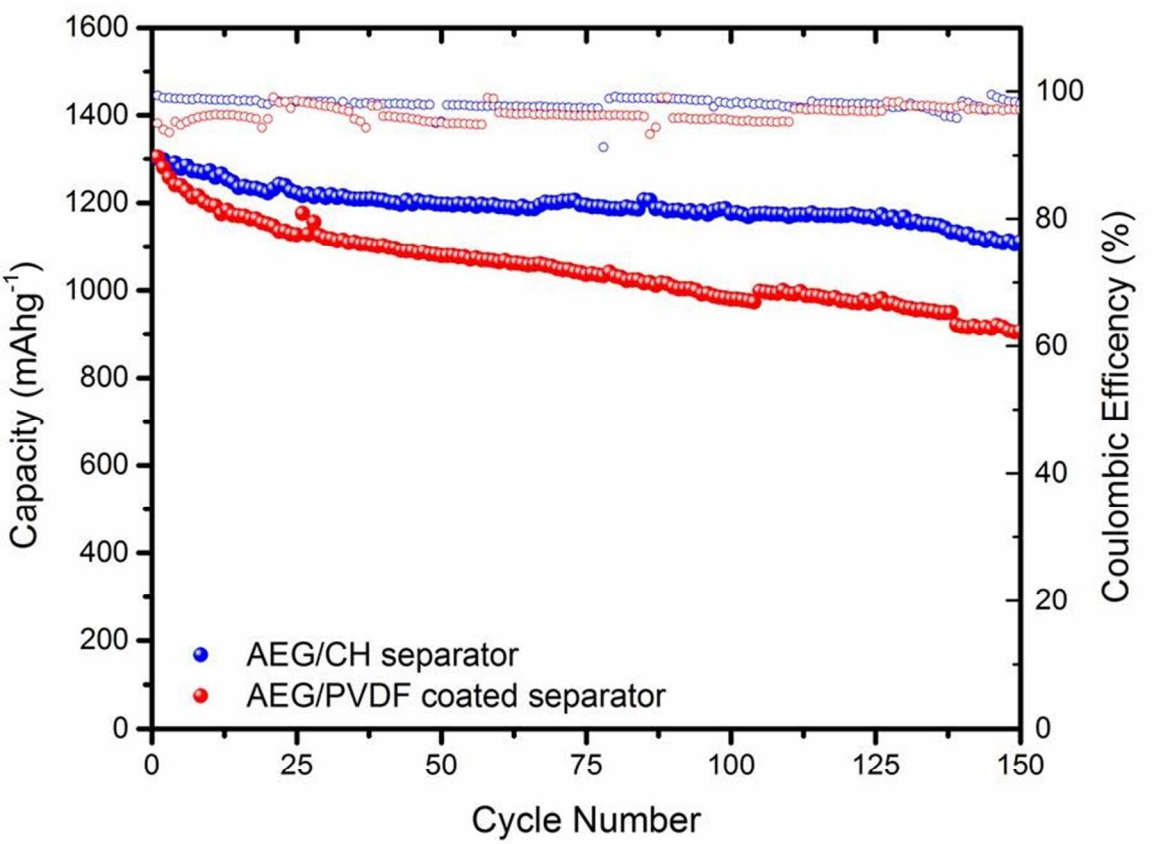

Figure S2. Cycling performance of Li–S cells incorporating AEG/PVDF- and AEG/CH-coated separators at a current rate of 0.1 C (1C = 1670 mA g^{-1}).

Fig S2 compares the cycle lives of the AEG/CH-coated separator and the AEG/PVDF coated separator; we attribute the greater capacity retention in the former to the presence of the CH binder in the AEG matrix and its chemical interactions with the LiPSs.

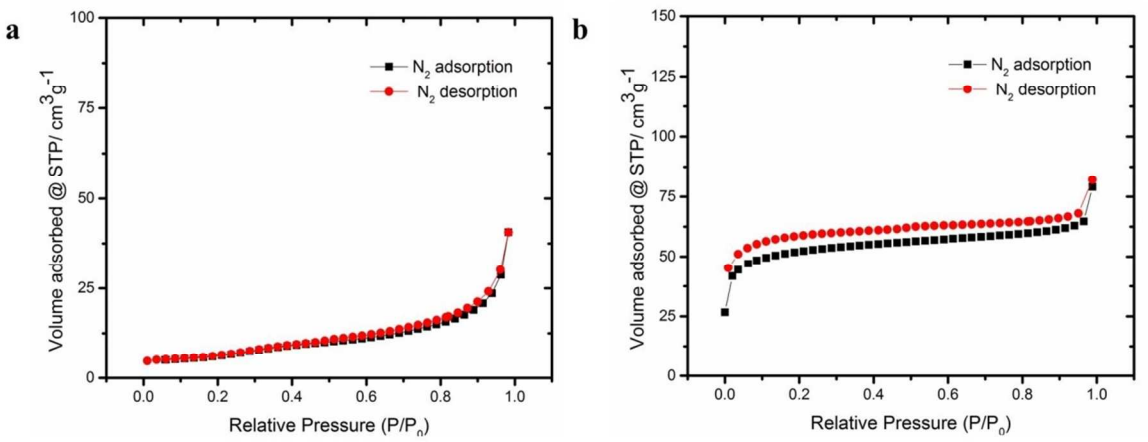

Figure S3. (a) N_2 Sorption isotherm of EG flakes. (b) N_2 Sorption isotherm of AEG flakes.

Table S1

Surface area, micro-pore and cumulative volume comparison of EG and AEG flakes

Sample name	Surface area (m^2g^{-1})	Micro-pore volume[a] (cm^3g^{-1})	Cumulative volume[b] (cm^3g^{-1})
EG	23	0.0039	0.068
AEG	368	0.102214	0.077

[a] t-Plot micro pore volume.

[b] BJH desorption cumulative volume of pores between 1.7000 nm and 300.0000 nm

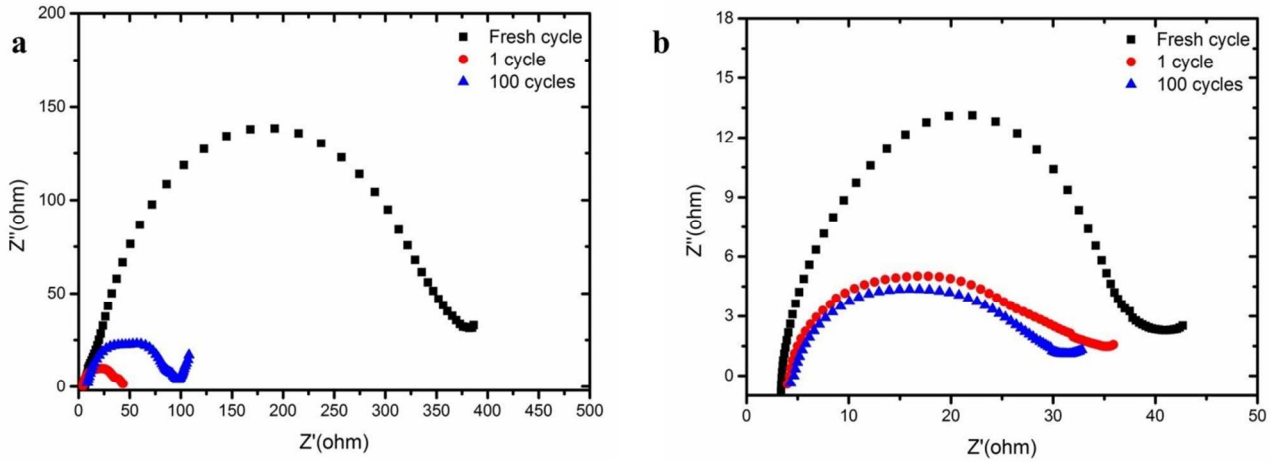

Figure S4. Electrochemical impedance spectra of Li–S cells (fresh and after 1st and 100th cycles) incorporating (a) pristine and (b) AEG/CH-coated separators.

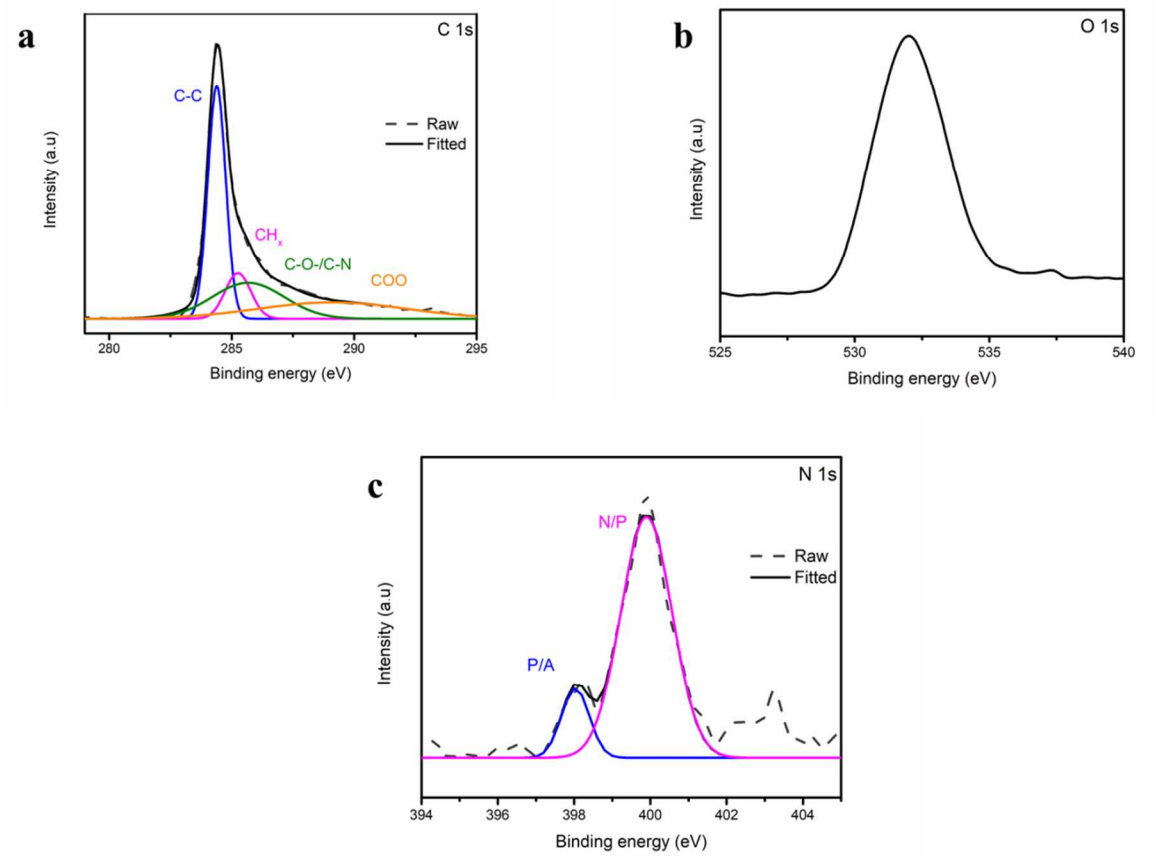

Figure S5. XPS spectra of AEG including C 1s, O 1s and N 1s regions.

Table S2

Elemental analysis of AEG flakes acquired from XPS survey spectra

Sample	C %	N %	O %
AEG	91.1 ± 0.1	0.2 ± 0.1	8.7 ± 0.1

XPS characterization of AEG flakes was performed to access the elemental composition. The high resolution spectra of carbon (C), oxygen (O) and nitrogen (N) is revealed in Fig S5 and further elemental analysis in table S2. The C 1s region in Fig S5 (a) was fitted by four major components attributed to graphitic carbon, hydrocarbons, alcoholic and/ or carbon nitrogen structures and ester or carboxyl.[1, 2] O 1s in Fig S5 (b) was fitted with only one component related to C-O bond. Finally N 1s region in Fig S5 (c) was fitted by two components related to pyridine/amine and/or Nitrite/pyrrole.

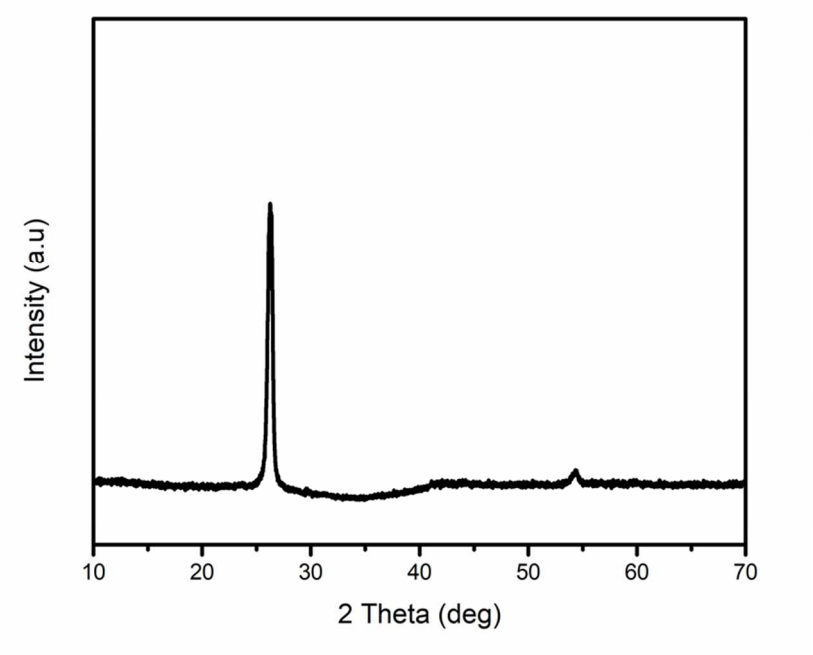

Figure S6. X-ray diffraction pattern of AEG flakes.

The X-ray diffraction was done to examine the crystallinity after activation process. The AEG exhibits sharp diffraction peak centered at 26.5º relating to (0 0 2) graphite plane, hence confirming the material obtained is indeed carbon.

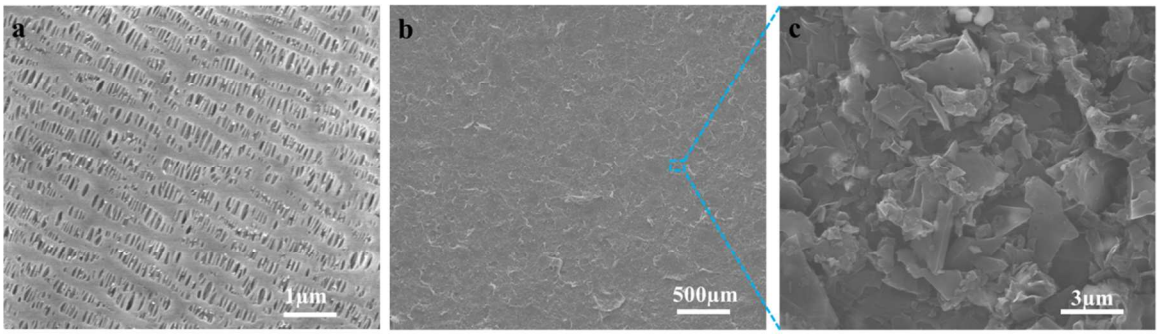

Figure S7. (a) SEM image of pristine separator. (b.c) SEM images of AEG/CH coated on top of separator.

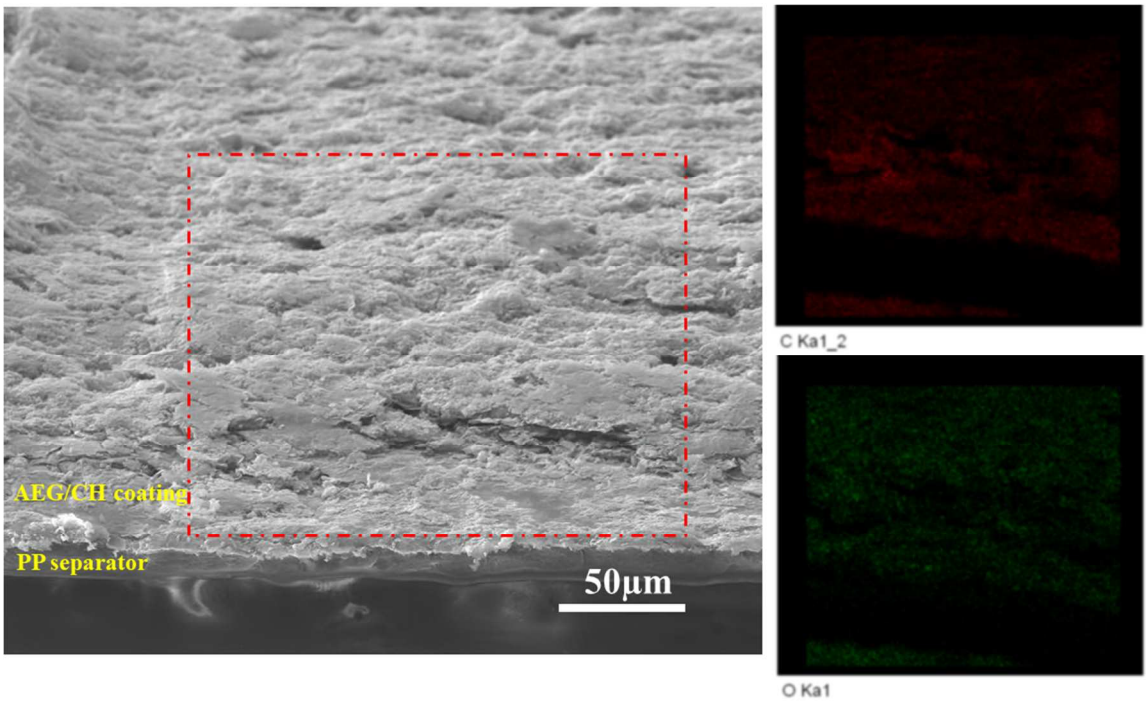

Figure S8. Tilt angle SEM image of fresh AEG/CH coated separator and corresponding EDX mapping.

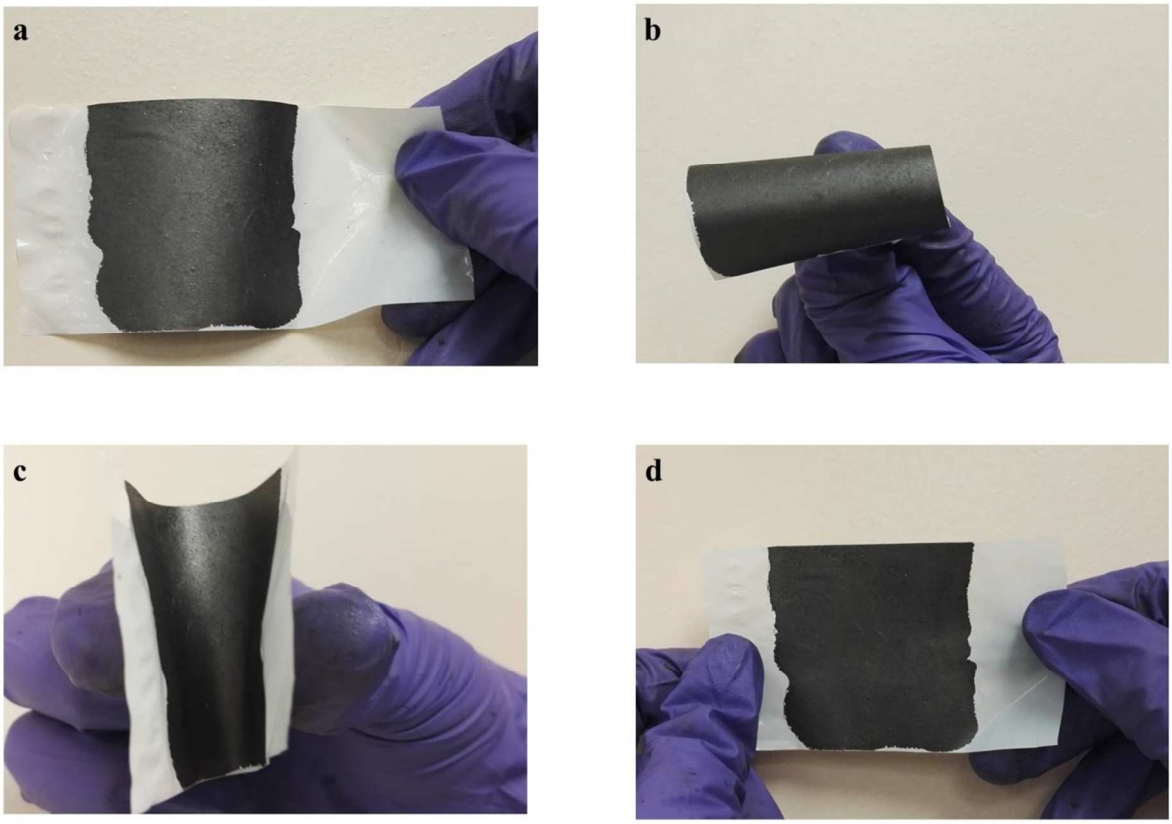

Figure S9. Photographs of the AEG/CH-coated separator in (a) flat, (b, c) bent, and (d) flat states.

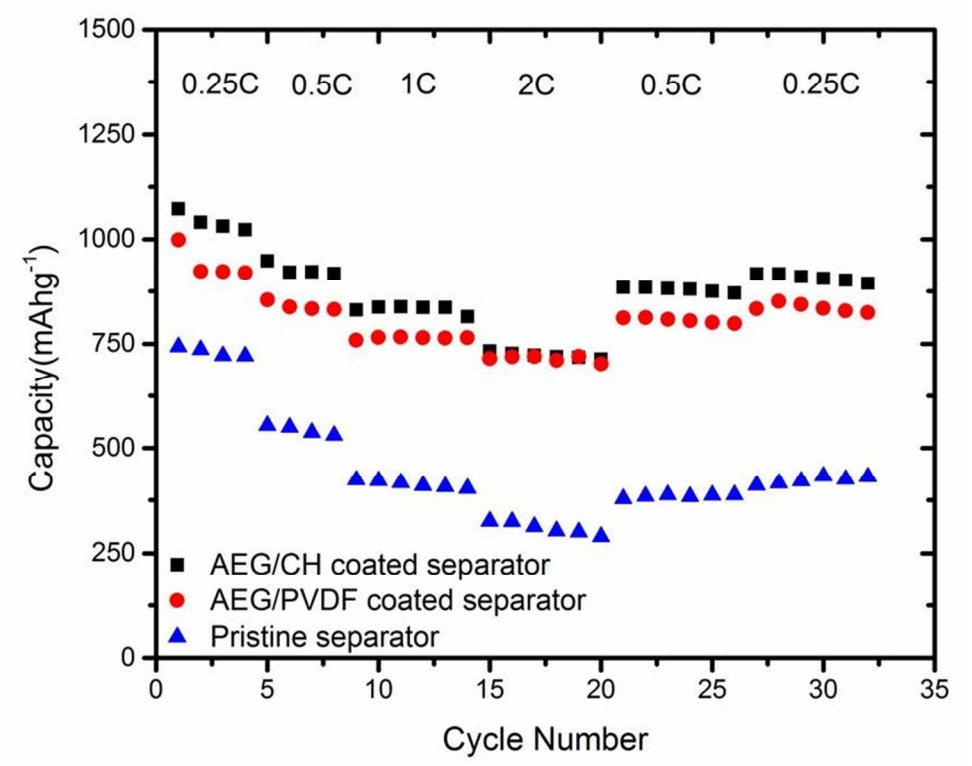

Figure S10. Comparison of the C-rate tests of pristine, AEG/CH- and AEG/PVDF-coated separators.

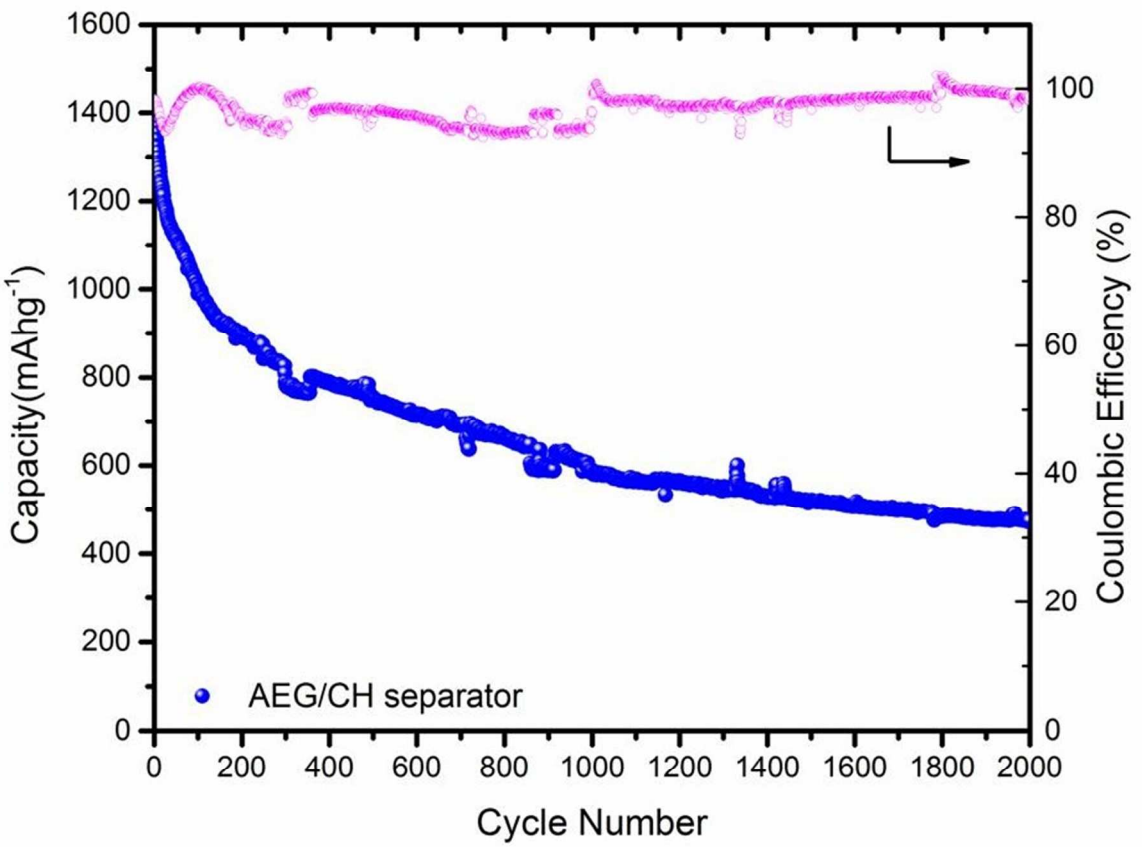

Figure S11. Cycle life test of a Li–S battery incorporating the AEG/CH-coated separator at 0.25C.

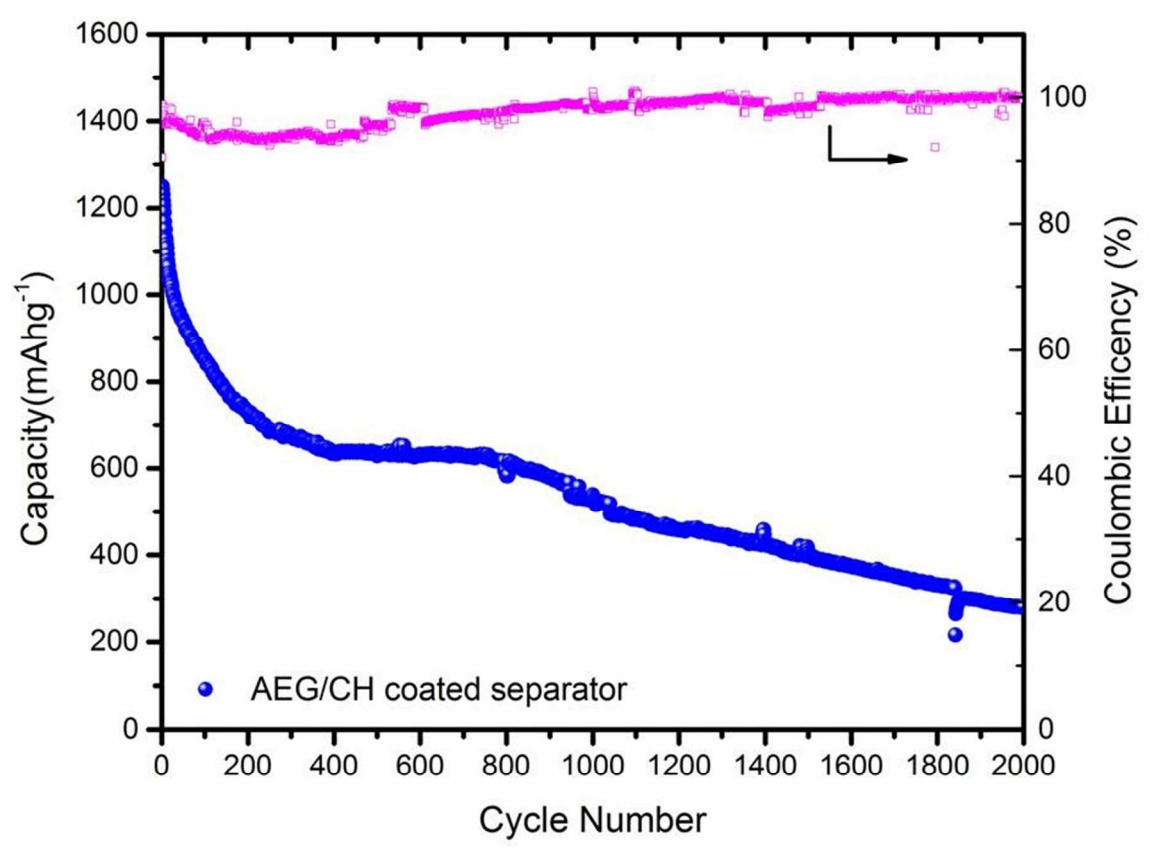

Figure S12. Cycle life test of the Li-S battery incorporating the AEG/CH-coated separator at 0.5C.

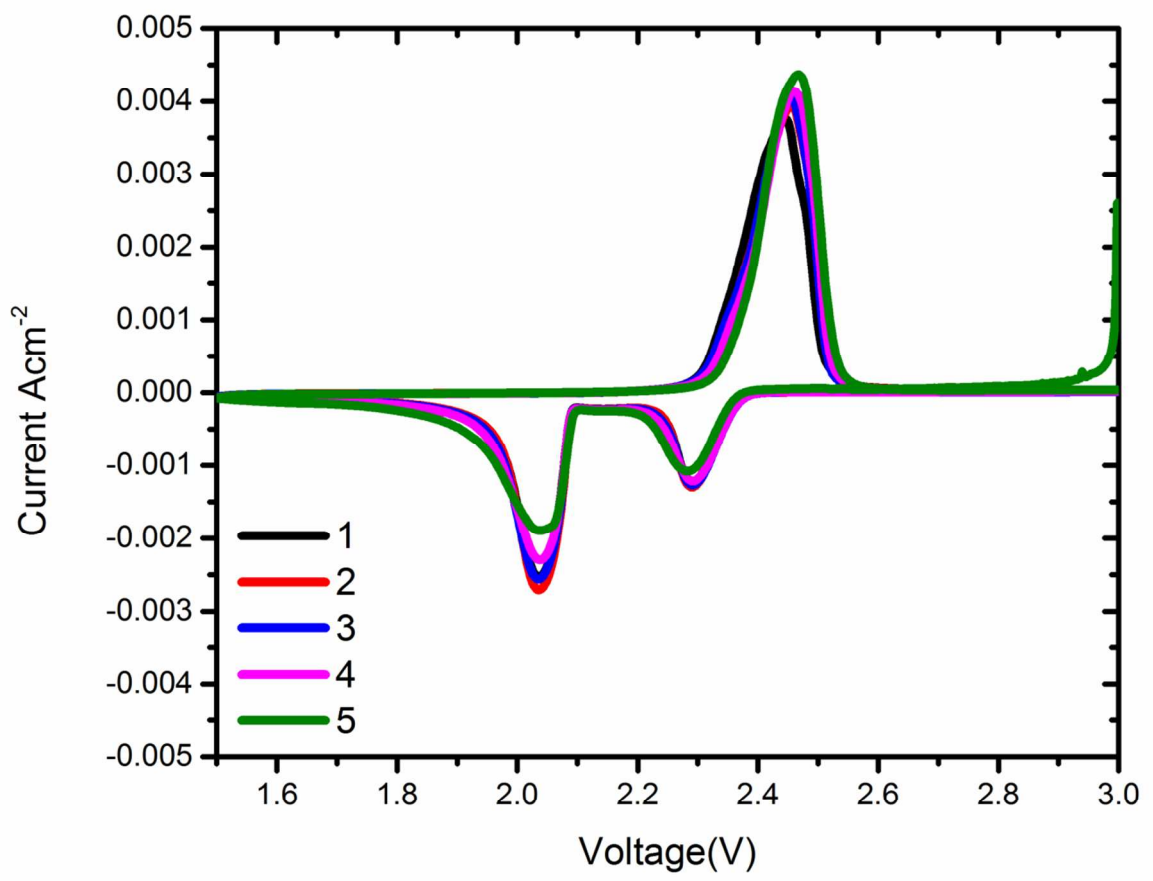

Figure S13. Continuous CV traces (scan rate: 0.1 mV s^{-1}) of the Li–S cell incorporating the pristine separator.

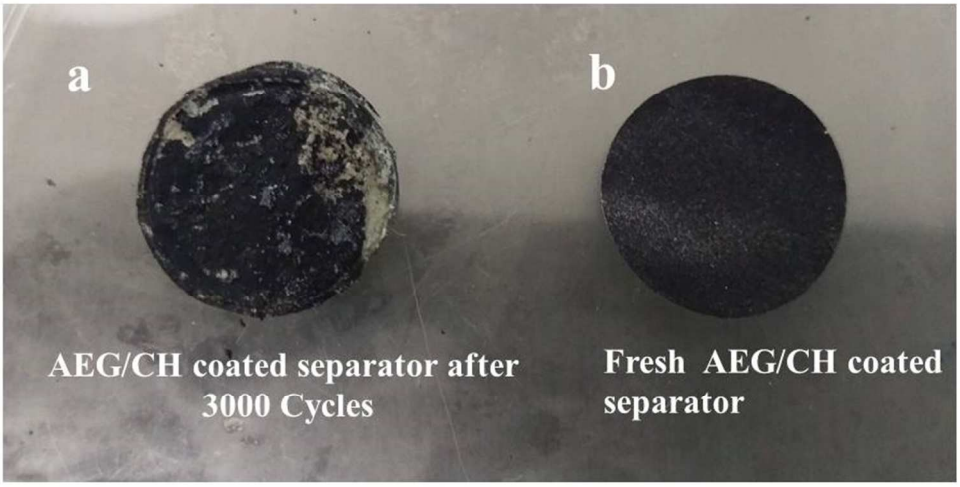

Figure S14. Photograph of (a) a separator after 3000 cycles (a large proportion of the AEG/CH coating remains intact) and (b) a freshly prepared AEG/CH-coated separator.

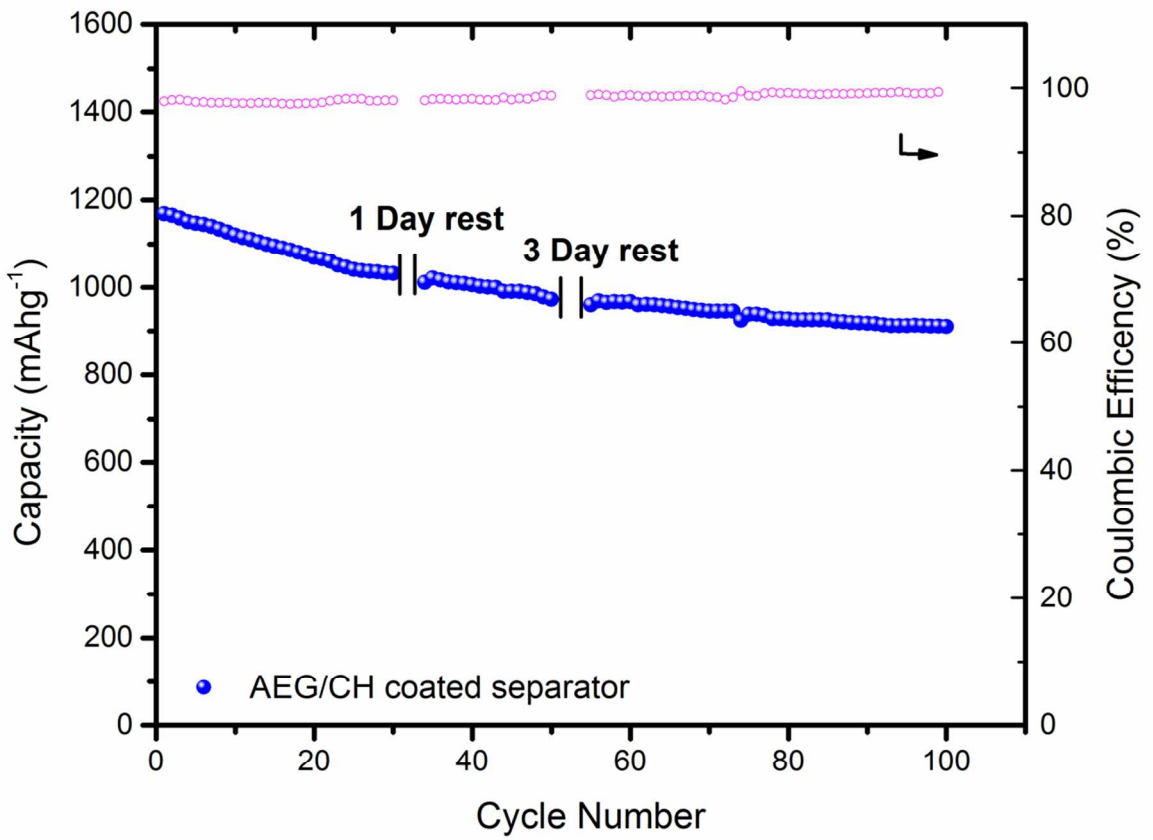

Figure S15. Rest test (1 and 3 days) of a Li–S cell incorporating the AEG/CH-coated separator, at a current density of 0.5C.

Rest test of Li-S battery based on AEG/CH separator was performed for 1 and 3 days in order to see the self-discharge effect. 1.5 % loss after 1st day and 1.1% loss after 3days of rest were detected.

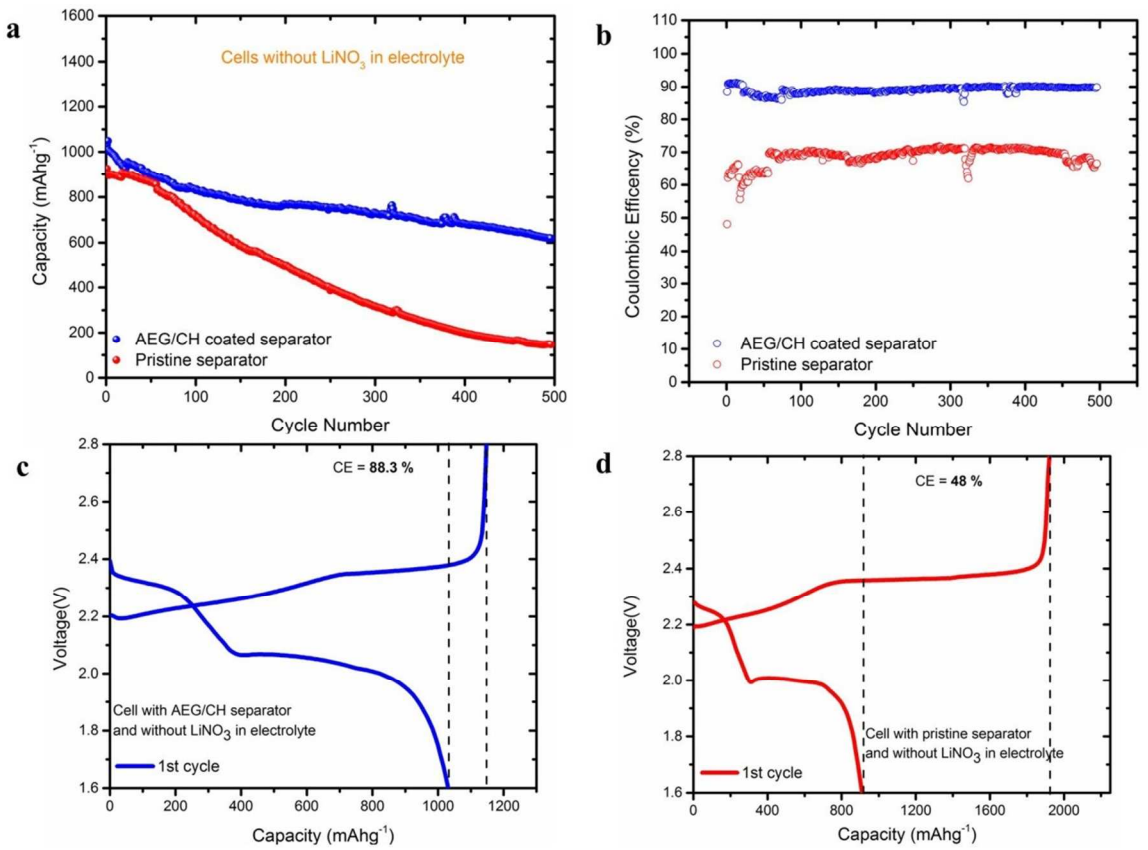

Figure S16. (a) Cycling performance of conventional Li–S cells incorporating pristine and AEG/CH-coated separators, recorded without $LiNO_3$ in the electrolyte at 0.5C. (b) Coulombic efficiencies of pristine and AEG/CH-coated separators. (c, d) Discharge/charge profiles of (c) AEG/CH-coated and (d) pristine separators in the first cycle, recorded without $LiNO_3$ in the electrolyte.

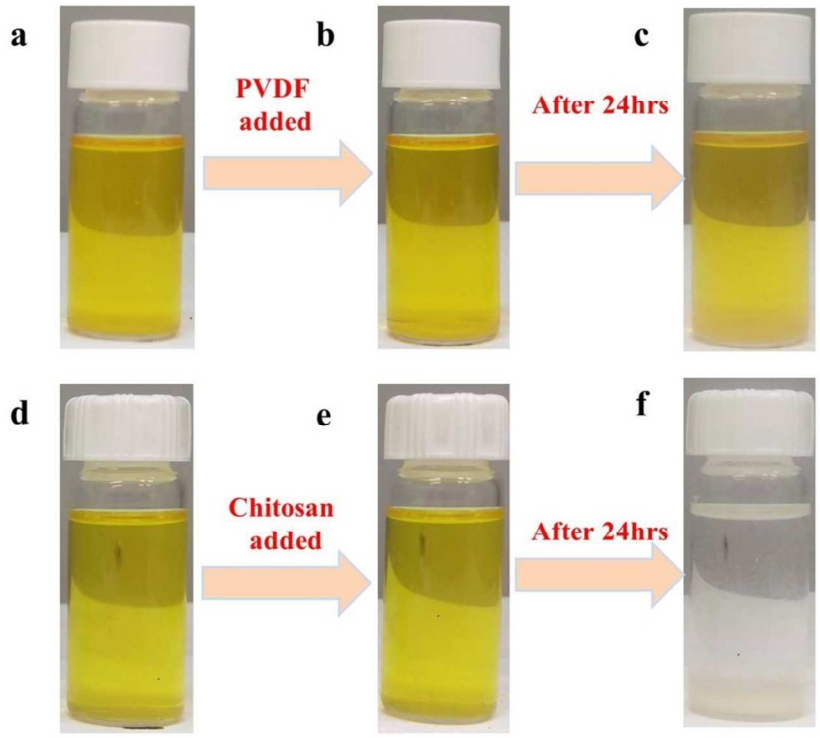

Figure S17. (a,d) LiPS (Li_2S_6) solution in DOL/DME (1:1). (b,e) PVDF and Chitosan added to the LiPS solution in (c,f) soaked in the LiPS solution for 24 h .

A lithium polysulfide solution (Li_2S_6) was prepared by mixing appropriate ratios of sulfur powder and Li_2S in a DOL/DME (1 : 1, v/v) solution for 24 h. 100µl of Li_2S_6 solution was further added in 5ml DOL/DME (1 : 1, v/v) to make dilute solution as shown in (Fig S13 a, d) along with 0.1 g of PVDF and Chitosan as shown in (Fig S13 b, e) to see the polysulfide adsorption. Images in (Fig S13 c, f) suggest that the chitosan is very much effective for adsorption of LiPSs compared to PVDF.

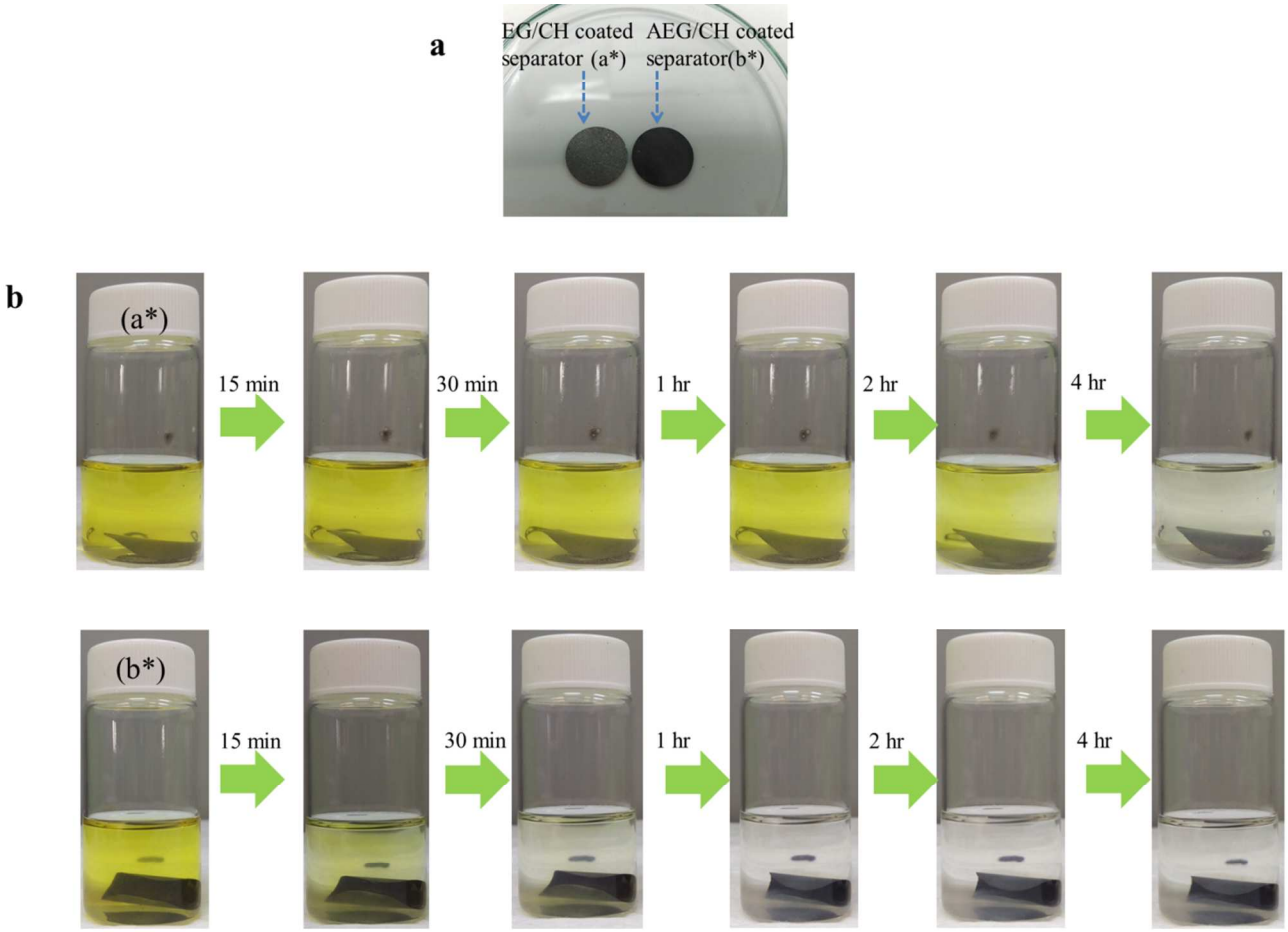

Figure S18. (a) Photograph of EG/CH coated separator denoted as a* and AEG/CH coated separator denoted as b*. (b) Lithium polysulfide capturing ability of both EG/CH and AEG/CH coated separator is shown relative to time.

Amount of material loaded on both separators (AEG/CH and EG/CH) was ~0.13mg cm^2. 300µl of Li_2S_6 solution was further added in 6ml DOL/DME (1 : 1, v/v) solution and both separators were added in to individual bottles at the same time. Photographic evidence concludes that the EG/CH coated separator adsorbs the lithium polysulfide in four hours, However the lithium polysulfide capturing ability is significantly enhanced in case of AEG/CH coated separator and solution turns color less in just one hour, Hence increasing the rate of lithium polysulfide capture by four. We attribute the enhancement in lithium polysulfide capture to high surface area of 368 $m^2g^{-1}$of AEG compared to EG 23 m^2g^{-1}.

Table S3 Comparison of long-term cycling stability in this study with some of the best reported for advanced Li–S battery systems using a modified polypropylene separator.

Type of coating on separator	Initial capacity (mA h g^{-1})	Final capacity (mA h g^{-1})	Current rate (mA h g^{-1})	Number of cycles	Fading rate per cycle (%)	S loading (mg cm^{-2})	S content (wt%)	Ref
Graphene coating	1000	680	1C	300	0.106	3–4	–	[3]
Carbon black coating	1306	810	0.5C	200	0.19	1.1–1.3	55	[4]
Microporous carbon coating	1214	503	0.2C	500	0.117	2.0	65	[5]
Microporous/ PEG coating	1307	596	0.2C	500	0.109	2.0	65	[5]
MWCNT coating	1073	621	1C	300	0.14	2.0	65	[6]
PVDF KOH activated CB	1150	669	0.5C	500	0.084	7.0	70	[7]
PVDF CB coating	1350	740	0.2C	500	0.09	1.5–2	50	[8]
Meso carbon coating	1060	683	1C	500	0.071	1.5–1.6	50	[9]
PEDOT:PSS coating	914	682	0.25C	600	0.042	0.09–1.1	64	[10]
MoS_2 coating	808	401	0.5C	600	0.083	–	65	[11]
$BaTiO_3$ coating	1122	929.5	0.1C	50	0.034	3	60	[12]

Black phosphorous coating	930	800	0.2C	100	0.14	1.5–2	80	[13]
COF-CNT coating	ca. 1130	ca. 650	0.2C	300	0.13	1.1	75	[14]
Nafion coating	781	ca. 468.6	0.5C	500	0.08	0.53	50	[15]
Silica nanoparticles coating	937	603	0.2C	200	0.175	1.2–1.4	48	[16]
$Ca(OH)_2$-carbon coating	1215	873.5	0.5C	250	ca. 0.11	1.2–1.5	63	[17]
AEG/CH coating	**1264**	**498**	**1C**	**3000**	**0.021**	**1.6–2**	**75**	**This work**

References

1. Terzyk, A. P. The Influence of Activated Carbon Surface Chemical Composition on the Adsorption of Acetaminophen (paracetamol) in Vitro: Part II. TG, FTIR, and XPS Analysis of Carbons and the Temperature Dependence of Adsorption Kinetics at the Neutral pH. *Colloids Surf. A.* **2001**, 177, 23-45.
2. Barzegar, F.; Bello, A.; Momodu, D.; Madito, M. J.; Dangbegnon, J.; Manyala, N. Preparation and Characterization of Porous Carbon from Expanded Graphite for High Energy Density Supercapacitor in Aqueous Electrolyte. *J. Power Sources.* **2016**, 309, 245-253.
3. Zhou, G.; Pei, S.; Li, L.; Wang, D.-W.; Wang, S.; Huang, K.; Yin, L.-C.; Li, F.; Cheng, H.-M. A Graphene–Pure-Sulfur Sandwich Structure for Ultrafast, Long-Life Lithium–Sulfur Batteries. *Adv. Mater.***2014**, 26, 625-631.
4. Chung, S.-H.; Manthiram, A. Bifunctional Separator with a Light-Weight Carbon-Coating for Dynamically and Statically Stable Lithium-Sulfur Batteries. *Adv. Funct. Mater.* **2014**, 24, 5299-5306.
5. Chung, S.-H.; Manthiram, A. A Polyethylene Glycol-Supported Microporous Carbon Coating as a Polysulfide Trap for Utilizing Pure Sulfur Cathodes in Lithium–Sulfur Batteries. *Adv. Mater.***2014**, 26, 7352-7357.
6. Chung, S.-H.; Manthiram, A. High-Performance Li–S Batteries with an Ultra-lightweight MWCNT-Coated Separator. *J Phys Chem Lett.* **2014**, 5, 1978-1983.
7. He, G.; Hart, C. J.; Liang, X.; Garsuch, A.; Nazar, L. F. Stable Cycling of a Scalable Graphene-Encapsulated Nanocomposite for Lithium–Sulfur Batteries. *ACS Appl. Mater. Interfaces.* **2014**, 6, 10917-10923.
8. Yao, H.; Yan, K.; Li, W.; Zheng, G.; Kong, D.; Seh, Z. W.; Narasimhan, V. K.; Liang, Z.; Cui, Y. Improved Lithium-Sulfur Batteries with a Conductive Coating on the Separator to Prevent the Accumulation of Inactive S-related Species at the Cathode-Separator Interface. *Energy Environ. Sci.* **2014**, 7, 3381-3390.
9. Balach, J.; Jaumann, T.; Klose, M.; Oswald, S.; Eckert, J.; Giebeler, L. Functional Mesoporous Carbon-Coated Separator for Long-Life, High-Energy Lithium–Sulfur Batteries. *Adv. Funct. Mater.* **2015**, 25, 5285-5291.
10. Abbas, S. A.; Ibrahem, M. A.; Hu, L.-H.; Lin, C.-N.; Fang, J.; Boopathi, K. M.; Wang, P.-C.; Li, L.-J.; Chu, C.-W. Bifunctional Separator as a Polysulfide Mediator for Highly Stable Li-S Batteries. *J. Mater. Chem. A.* **2016**, 4, 9661-9669.
11. Ghazi, Z. A.; He, X.; Khattak, A. M.; Khan, N. A.; Liang, B.; Iqbal, A.; Wang, J.; Sin, H.; Li, L.; Tang, Z. MoS2/Celgard Separator as Efficient Polysulfide Barrier for Long-Life Lithium–Sulfur Batteries. *Adv. Mater.* **2017**, 10.1002/adma.201606817
12. Yim, T.; Han, S. H.; Park, N. H.; Park, M.-S.; Lee, J. H.; Shin, J.; Choi, J. W.; Jung, Y.; Jo, Y. N.; Yu, J.-S.; Kim, K. J. Effective Polysulfide Rejection by Dipole-Aligned BaTiO3 Coated Separator in Lithium–Sulfur Batteries. *Adv. Funct. Mater.* **2016**, 26, 7817-7823.
13. Sun, J.; Sun, Y.; Pasta, M.; Zhou, G.; Li, Y.; Liu, W.; Xiong, F.; Cui, Y. Entrapment of Polysulfides by a Black-Phosphorus-Modified Separator for Lithium–Sulfur Batteries. *Adv. Mater.* **2016**, 28, 9797-9803.

14. Yoo, J.; Cho, S.-J.; Jung, G. Y.; Kim, S. H.; Choi, K.-H.; Kim, J.-H.; Lee, C. K.; Kwak, S. K.; Lee, S.-Y. COF-Net on CNT-Net as a Molecularly Designed, Hierarchical Porous Chemical Trap for Polysulfides in Lithium–Sulfur Batteries. *Nano Lett.* **2016**, 16, 3292-3300.
15. Huang, J.-Q.; Zhang, Q.; Peng, H.-J.; Liu, X.-Y.; Qian, W.-Z.; Wei, F. Ionic Shield for Polysulfides Towards Highly-stable Lithium-Sulfur Batteries. *Energy Environ. Sci.* **2014**, 7, 347-353.
16. Li, J.; Huang, Y.; Zhang, S.; Jia, W.; Wang, X.; Guo, Y.; Jia, D.; Wang, L. Decoration of Silica Nanoparticles on Polypropylene Separator for Lithium–Sulfur Batteries. *ACS Appl. Mater. Interfaces.* **2017**, 9, 7499-7504.
17. Shao, H.; Huang, B.; Liu, N.; Wang, W.; Zhang, H.; Wang, A.; Wang, F.; Huang, Y. Modified Separators Coated with a Ca(OH)2-carbon Framework Derived from Crab Shells for Lithium-Sulfur Batteries. *J. Mater. Chem. A.* **2016**, 4, 16627-16634.